

# Magnetostructural correlations and catecholase-like activities of $\mu$ -alkoxo-bridged dinuclear copper(II) complexes with 1-diethylaminopropan-2-ol, $\text{N}_3^-$ , $\text{NCO}^-$ and $\text{NO}_2^-$ ligands †

Yun-Ho Chung,<sup>a</sup> Ho-Hsiang Wei,<sup>\*a</sup> Yi-Hung Liu,<sup>b</sup> Gene-Hsiang Lee<sup>b</sup> and Yu Wang<sup>b</sup>

<sup>a</sup> Department of Chemistry, Tamkang University, Tamsui, Taiwan

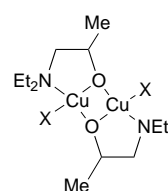
<sup>b</sup> Instrumentation Center, College of Science, National Taiwan University, Taipei, Taiwan

Three new  $\mu$ -alkoxo-bridged dinuclear copper(II) complexes with  $\mu$ -1-diethylaminopropan-2-olate,  $[\text{Cu}_2\{\mu\text{-Et}_2\text{N-CH}_2\text{CH}(\text{Me})\text{O}\}_2\text{X}_2]$  ( $\text{X} = \text{N}_3^-$  **1**,  $\text{NCO}^-$  **2** or  $\text{NO}_2^-$  **3**), have been prepared and characterized by single-crystal X-ray diffraction analyses. The copper atoms have distorted square-planar environments bridged by two oxygen atoms of alkoxo groups. Magnetic susceptibility measurements in the temperature range 5–300 K indicated significant antiferromagnetic coupling for **3** and ferromagnetic coupling for **1** and **2** between the copper(II) atoms. The best least-squares-fitted coupling constants ( $2J$ ) for **1**, **2** and **3** were 81, 25 and  $-42 \text{ cm}^{-1}$  respectively. By comparison to the known complex  $[\text{Cu}_2\{\mu\text{-Et}_2\text{NCH}_2\text{CH}(\text{Me})\text{O}\}_2(\text{NCS})_2]$  **4** ( $2J = -86.0 \text{ cm}^{-1}$ ), a linear correlation between the magnetic coupling constants and the mean Cu–O–Cu angle ( $\varphi$ ) with a crossover point at  $\varphi 97.3^\circ$  from antiferromagnetic to ferromagnetic coupling is obtained. The catecholase activity of these copper(II) complexes for the oxidation of 3,5-di-*tert*-butylcatechol by  $\text{O}_2$  was studied and shown to be in the order **1** < **2** < **3**.

Dinuclear copper complexes play an important role in biological metalloenzymes.<sup>1–4</sup> The best investigated dinuclear copper(II) enzymes are hemocyanin,<sup>2</sup> and tyrosinase<sup>3</sup> or catecholase.<sup>4</sup> Tyrosinase catalyses the aerial oxidation of monophenols to *o*-diphenols (cresolase activity) and the oxidation of *o*-phenols (catechols) to *o*-quinones (catecholase activity). The crystal structure of tyrosinase has not been determined, but spectroscopic studies seem to reveal that the active site is similar to that of hemocyanin.<sup>3</sup> Extended X-ray absorption fine structure (EXAFS) measurements for the met-tyrosinase give a  $\text{Cu}\cdots\text{Cu}$  distance of 3.4 Å. Spectroscopic studies on the native met form of catecholase from *Lycopus* and *Ipomoea batatas* have revealed that the active site consists of two copper atoms with the  $\text{Cu}\cdots\text{Cu}$  distance of 2.9 Å, where the metals are co-ordinated by four N/O donor ligands.<sup>4</sup>

Particular interest has been directed towards the magnetic coupling phenomena and the catalytic activities in biological model dinuclear copper(II) complexes. In studies of the cryomagnetic behaviours of dinuclear copper(II) complexes it is important to examine them with reference to the magnetostructural criteria which have been established on similar copper(II) dimers.<sup>5</sup> A linear relationship between the magnetic coupling constant ( $2J$ ) and the Cu–O–Cu bridging angle ( $\varphi$ ) was first established in a series of symmetrically bridged copper(II) hydroxide complexes by Hodgson and co-workers.<sup>6</sup> Recently, several reports on the linear relationship between  $2J$  and the Cu–O–Cu bridging angle have appeared concerning dinuclear copper(II) complexes with dialkoxo,<sup>7</sup> heterocyclic thione,<sup>8</sup>  $\mu$ -hydroxo- $\mu$ -carboxylato,<sup>9</sup>  $\mu$ -phenoxide<sup>10</sup> and carboxylato<sup>11</sup> bridging ligands. For dihydroxo-bridged dicopper(II) complexes,<sup>6</sup> in which the crossover from ferromagnetic to antiferromagnetic behaviour occurs at about Cu–O–Cu  $97.5^\circ$ , it is not certain how extensive these might be.

We have been particularly interested in dinuclear copper(II) complexes as structural and functional models for catecholase, and further to investigate the magnetostructural correlation between  $2J$  and Cu–O–Cu bridging angle, we prepared a series of dinuclear copper(II) complexes with  $\mu$ -1-diethyl-



$\text{X} = \text{N}_3^-(1), \text{NCO}^-(2), \text{NO}_2^-(3)$

Scheme 1

aminopropan-2-olate bridging ligands (Scheme 1),  $[\text{Cu}_2\{\mu\text{-Et}_2\text{NCH}_2\text{CH}(\text{Me})\text{O}\}_2\text{X}_2]$ , where  $\text{X} = \text{N}_3^-$  **1**,  $\text{NCO}^-$  **2** or  $\text{NO}_2^-$  **3**. In general, a way to get a short metal–metal distance in a model dicopper(II) complex, which is close to the  $\text{Cu}\cdots\text{Cu}$  distance of 2.9 Å in native catecholase, and enables strong magnetic coupling, is by using dinucleating ligands with a bridging alcoholate or phenolate oxygen atom. Up to now, crystal structure and magnetic studies of dinuclear copper(II) complexes with  $\mu$ -1-diethylaminopropan-2-olate ligands have been limited to only  $[\text{Cu}_2\{\mu\text{-Et}_2\text{NCH}_2\text{CH}(\text{Me})\text{O}\}_2(\text{NCS})_2]$ .<sup>12</sup> In the present paper, emphasis has been placed on the effect of the anionic ligands  $\text{X}^-$  on the magnetostructural correlations and the catalytic activity of the oxidation of 3,5-di-*tert*-butylcatechol with  $\text{O}_2$  for these three new copper(II) complexes, **1–3**.

## Experimental

### Preparation of compounds

**[Cu<sub>2</sub>{μ-Et<sub>2</sub>NCH<sub>2</sub>CH(Me)O}<sub>2</sub>(N<sub>3</sub>)<sub>2</sub>] 1.** To a methanolic solution (20 cm<sup>3</sup>) of 1-diethylaminopropan-2-ol (404 mg, 3.08 mmol) and copper(II) acetate monohydrate (200 mg, 1.02 mmol), a methanol solution (10 cm<sup>3</sup>) of sodium azide (66.4 mg, 1.02 mmol) was added. The reaction mixture was allowed to stand at 25 °C for several days. Dark black single crystals formed, and were filtered off and dried *in vacuo*. Yield 82% (Found: C, 35.2; H, 6.6; N, 23.6. Calc.: C, 35.7; H, 6.8; N, 23.8%). IR (KBr disc):  $\nu(\text{N}_3^-)$  2045 and 2056 cm<sup>-1</sup>.

**[Cu<sub>2</sub>{μ-Et<sub>2</sub>NCH<sub>2</sub>CH(Me)O}<sub>2</sub>(NCO)<sub>2</sub>] 2.** This complex was prepared in a similar manner to that of **1**, but where  $\text{NaN}_3$  was replaced by KNCO. Dark green single crystals were formed.

† Non-SI unit employed:  $\mu_B \approx 9.27 \times 10^{-24} \text{ J T}^{-1}$ .

Yield 85% (Found: C, 40.5; H, 6.8; N, 11.4. Calc.: C, 40.8; H, 6.8; N, 11.3%). IR (KBr disc):  $\nu(\text{NCO}^-)$  2220  $\text{cm}^{-1}$ .

**[Cu<sub>2</sub>{ $\mu$ -Et<sub>2</sub>NCH<sub>2</sub>CH(Me)O}<sub>2</sub>(NO<sub>2</sub>)<sub>2</sub>] 3.** This complex was prepared in similar manner to that of **1**, but where NaN<sub>3</sub> was replaced by NaNO<sub>2</sub>. Dark green crystals formed. Yield 75% (Found: C, 32.9; H, 6.8; N, 11.2. Calc.: C, 32.6; H, 7.0; N, 11.0%). IR (KBr disc):  $\nu(\text{NO}_2^-)$  1456 and 1381  $\text{cm}^{-1}$ .

### Physical measurements

The IR spectra were recorded on a Bio-Rad FTS40 FTIR spectrophotometer as KBr pellets in the 4000–400  $\text{cm}^{-1}$  region, X-band EPR spectra at 300 K for the complexes as powders on a Bruker ESC-106 spectrometer. The temperature dependence of the magnetic susceptibility of polycrystalline samples was measured between 5 and 300 K at a field of 1 T using a Quantum Design model MPMS computer-controlled SQUID magnetometer. Diamagnetic corrections were made using Pascal's constants.<sup>13</sup> Electronic spectra were recorded on a Shimadzu PC-3101 spectrophotometer.

### Crystallography

**Crystal data.** **Complex 1.** C<sub>14</sub>H<sub>32</sub>Cu<sub>2</sub>N<sub>8</sub>O<sub>2</sub>, *M* = 471.55, monoclinic, space group *P*2<sub>1</sub>/*n*, *a* = 11.995(4), *b* = 14.033(3), *c* = 13.1928(18) Å,  $\beta$  = 104.173(18)°, *U* = 2153.1(8) Å<sup>3</sup>, *D<sub>c</sub>* (*Z* = 4) = 1.455 g cm<sup>-3</sup>, *F*(000) = 987,  $\mu$  = 20.046 cm<sup>-1</sup>, crystal size 0.13 × 0.35 × 0.43 mm,  $2\theta_{\text{max}}$  = 50°, *N* = 3777, *N<sub>o</sub>* = 2532, *R* = 0.032, *R'* = 0.032.

**Complex 2.** C<sub>16</sub>H<sub>32</sub>Cu<sub>2</sub>N<sub>4</sub>O<sub>4</sub>, *M* = 471.54, monoclinic, space group *P*2<sub>1</sub>/*c*, *a* = 13.3108(21), *b* = 9.3876(12), *c* = 18.4407(17) Å,  $\beta$  = 110.211(10)°, *U* = 2162.4(5) Å<sup>3</sup>, *D<sub>c</sub>* (*Z* = 4) = 1.448 g cm<sup>-3</sup>, *F*(000) = 987,  $\mu$  = 53.247 cm<sup>-1</sup>, crystal size 0.30 × 0.35 × 0.35 mm,  $2\theta_{\text{max}}$  = 50°, *N* = 3795, *N<sub>o</sub>* = 2698, *R* = 0.030, *R'* = 0.031.

**Complex 3.** C<sub>14</sub>H<sub>32</sub>Cu<sub>2</sub>N<sub>4</sub>O<sub>6</sub>, *M* = 479.52, monoclinic, space group *P*2<sub>1</sub>/*c*, *a* = 10.281(23), *b* = 13.078(4), *c* = 8.0038(23) Å,  $\beta$  = 92.068(21)°, *U* = 1067.8(5) Å<sup>3</sup>, *D<sub>c</sub>* (*Z* = 2) = 1.491 g cm<sup>-3</sup>, *F*(000) = 501,  $\mu$  = 20.415 cm<sup>-1</sup>, crystal size 0.4 × 0.50 × 0.50 mm,  $2\theta_{\text{max}}$  = 55°, *N* = 2458, *N<sub>o</sub>* = 1950, *R* = 0.028, *R'* = 0.036.

The X-ray crystal data were collected at room temperature using an Enraf-Nonius CAD4 diffractometer equipped with graphite-monochromated Mo-K $\alpha$  radiation ( $\lambda$  = 0.7107 Å),  $2\theta$ - $\theta$  scan mode. The *N* independent reflections and *N<sub>o</sub>* with *I* > 2.0 $\sigma$ (*I*) were observed. The structures were solved by location of heavy atoms using a Patterson map and refined (based on *F*) by a full-matrix least-squares method using the NRCVAX software package,<sup>14</sup> the function minimized was  $\sum w(|F_o| - |F_c|)^2$  and unit weights were used. All non-hydrogen atoms were readily located and refined with anisotropic thermal parameters; *R* =  $\sum |F_o - F_c| / \sum |F_o|$  and *R'* =  $(\sum w|F_o - F_c|^2 / \sum w|F_o|^2)^{1/2}$  respectively.

CCDC reference number 186/583.

### Catalytic activity for the oxidation of 3,5-di-*tert*-butylcatechol

Electronic spectra at 25 °C were recorded for complexes **1–3** and their catalytic activity for the oxidation of 3,5-di-*tert*-butylcatechol (H<sub>2</sub>dtbc) with O<sub>2</sub> monitored on a UV/VIS spectrophotometer. The reaction with H<sub>2</sub>dtbc was studied at 25 °C by adding quantitative catechol solutions to the same amounts of the complexes and recording the spectra at different time intervals. The yield of quinone formed in the oxidation in methanol was determined from the measured absorbances at about 400 nm of the resulting solutions.<sup>15</sup>

## Results and Discussion

### Syntheses and IR spectra of the complexes

The dinuclear copper(II) complexes **1**, **2** and **3** are obtained by reaction of NaN<sub>3</sub>, KNCO and NaNO<sub>2</sub>, respectively, with Cu(MeCO<sub>2</sub>)<sub>2</sub>·H<sub>2</sub>O and 1-diethylaminopropan-2-ol in aqueous

**Table 1** Selected bond distances (Å) and angles (°) for complex **1**

Cu(1)···Cu(2)	2.8067(7)	Cu(1)–O(1)	1.931(3)
Cu(1)–O(2)	1.9263(24)	Cu(2)–O(1)	1.9429(24)
Cu(2)–O(2)	1.9039(24)	Cu(1)–N(1)	2.041(3)
Cu(1)–N(3)	1.943(4)	Cu(2)–N(2)	2.048(3)
Cu(2)–N(6)	1.942(3)		
Cu(1)–O(1)–Cu(2)	92.86(11)	Cu(1)–O(2)–Cu(2)	94.24(10)
O(1)–Cu(1)–O(2)	78.33(13)	O(1)–Cu(2)–O(2)	78.57(10)
O(1)–Cu(2)–N(6)	101.33(13)	O(2)–Cu(1)–N(3)	102.15(14)
Cu(1)–N(3)–N(4)	121.4(3)	Cu(2)–N(6)–N(7)	123.4(3)
O(1)–Cu(1)–N(1)	85.49(11)	O(2)–Cu(2)–N(2)	85.33(13)

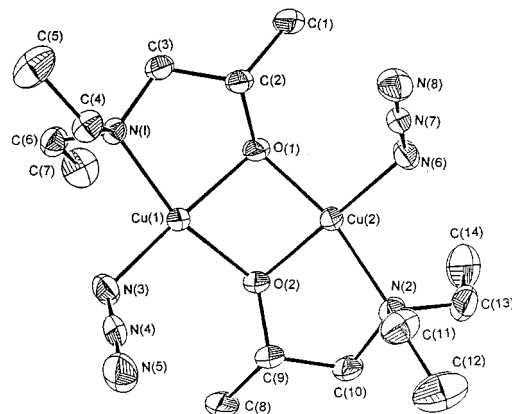


**Fig. 1** An ORTEP<sup>20</sup> view of complex **1** in the crystal showing the atomic numbering scheme (30% probability thermal ellipsoids)

methanol. The structural features of these complexes were determined by IR spectroscopy and single-crystal X-ray diffraction studies. The formulae are in accord with the elemental analyses. A strong doublet infrared absorption band at 2045 and 2056  $\text{cm}^{-1}$  for **1** is consistent with the asymmetric stretching of  $\nu(\text{N}_3^-)$  for terminal Cu–N<sub>3</sub> bonding.<sup>16</sup> The IR spectrum of complex **2** shows the asymmetric stretching band of  $\nu(\text{CN})$  at 2220  $\text{cm}^{-1}$ , corresponding to *N*-bonded terminal NCO<sup>-</sup>.<sup>17</sup> The IR spectrum of complex **3** contains two prominent asymmetric  $\nu(\text{NO}_2^-)$  stretches at 1456 and 1381  $\text{cm}^{-1}$ , which is characteristic of this type of nitrite complex.<sup>18,19</sup> These results are consistent with the X-ray diffraction studies.

### Crystal structures of complexes 1–3

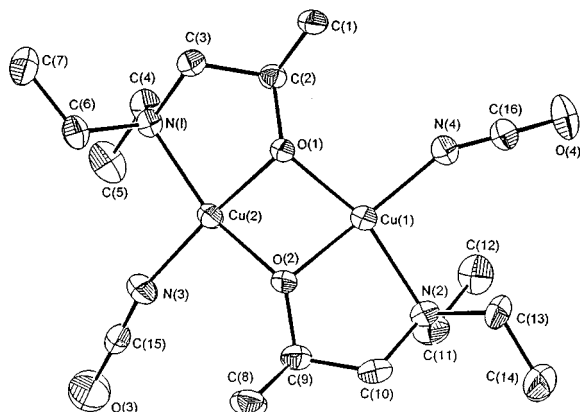
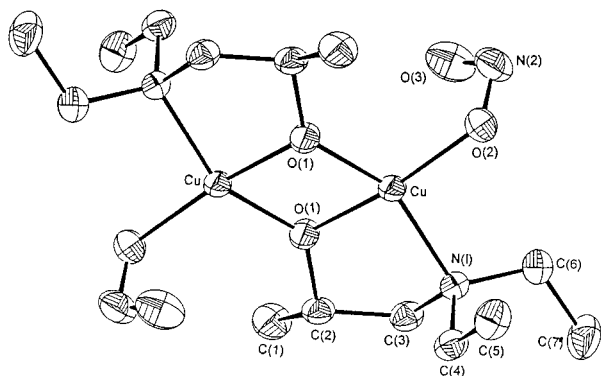
The overall structural characteristics for these three complexes **1–3** are substantially similar to those reported for [Cu<sub>2</sub>{ $\mu$ -Et<sub>2</sub>NCH<sub>2</sub>CH(Me)O}<sub>2</sub>(NCS)<sub>2</sub>] **4**.<sup>12</sup> Nevertheless, the structure of **4** consists essentially of  $\mu$ -alkoxo-bridged centrosymmetric dinuclear units. The dinuclear units are further bridged by thiocyanate groups to yield a one-dimensional chain. The Cu···Cu bond distance and the Cu–O–Cu bond angle in **4** are 2.975(1) Å and 100.4(3)° respectively.

The crystal structure of complex **1** is illustrated in Fig. 1 and bond distances and angles relevant to the copper co-ordination sphere are listed in Table 1. The co-ordination geometry around the copper atom is distorted square planar, and is formed by two  $\mu$ -alkoxo oxygen atoms, an amino nitrogen atom, and an azido nitrogen atom. The three nitrogen atoms of the azido group are as expected nearly collinear (176.7°). The azido group makes an average angle Cu–N–N of 122.4°; the bending may be due to hydrogen bonding between the hydrogen atoms of the methyl groups, C(1)H<sub>3</sub> or C(8)H<sub>3</sub>, and the nitrogen atoms N(5) and N(8). The Cu···Cu distance is 2.8067(7) Å and the average Cu–O–Cu angle is 93.55°.

The structure of complex **2** illustrated in Fig. 2 shows that each NCO<sup>-</sup> is nitrogen bonded to one copper atom. The square plane around the copper atoms is formed by two oxygen atoms

**Table 2** Selected bond distances (Å) and angles (°) for complex **2**

Cu(1)···Cu(2)	2.8690(22)	Cu(1)–O(1)	1.9090(22)
Cu(1)–O(2)	1.8905(22)	Cu(2)–O(1)	1.9483(22)
Cu(2)–O(2)	1.8905(22)	Cu(1)–N(1)	2.055(3)
Cu(1)–N(3)	1.905(4)	Cu(2)–N(2)	2.043(3)
Cu(2)–N(4)	1.877(3)		
Cu(1)–O(1)–Cu(2)	96.10(9)	Cu(1)–O(2)–Cu(2)	97.53(10)
O(1)–Cu(1)–N(1)	85.19(11)	O(2)–Cu(1)–N(3)	101.28(12)
O(2)–Cu(2)–N(2)	85.18(10)	O(1)–Cu(2)–N(4)	100.88(13)
N(1)–Cu(1)–N(3)	96.07(14)	N(2)–Cu(2)–N(4)	96.40(13)
O(1)–Cu(1)–O(2)	77.65(9)	O(1)–Cu(2)–O(2)	77.51(9)

**Fig. 2** An ORTEP view of complex **2** in the crystal. Details as in Fig. 1**Fig. 3** An ORTEP view of complex **3** in the crystal. Details as in Fig. 1

of the  $\mu$ -alkoxo-bridges and two nitrogen atoms from the ligand and  $\text{NCO}^-$ . The average angles of  $\text{Cu–O–Cu}$  and  $\text{Cu–N–C}$  [both  $\text{Cu(1)–N(4)–C(16)}$  and  $\text{Cu(2)–N(3)–C(15)}$ ] are  $96.77$  and  $165.65^\circ$  respectively. The  $\text{Cu}\cdots\text{Cu}$  distance is  $2.8690(22)$  Å (Table 2).

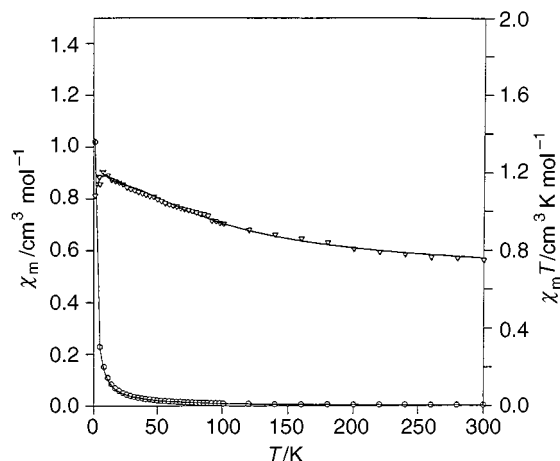
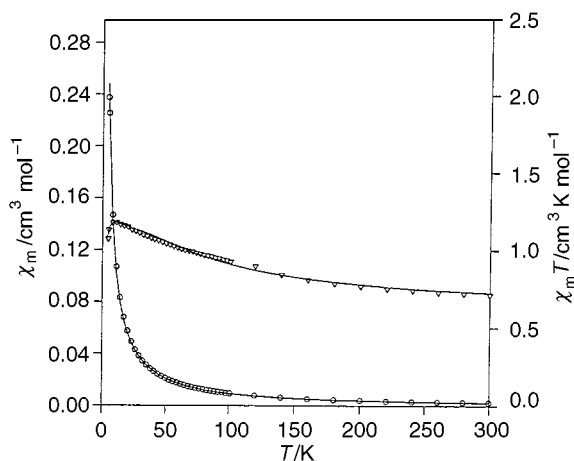
The structure of complex **3** as illustrated in Fig. 3 consists essentially of a  $\mu$ -alkoxo-bridged centrosymmetric dinuclear copper(II) unit. The nitrites bond to the copper atom through one oxygen atom [ $\text{Cu–O } 1.9664(25)$  Å] (Table 3). The nitrito groups are bent towards the copper atom and a second nitrite oxygen attempts to form five-co-ordination [ $\text{Cu}\cdots\text{O(3)} 2.495(3)$  Å]. Thus the  $\text{Cu}\cdots\text{Cu}$  distance,  $2.9279(10)$  Å, and the  $\text{Cu–O–Cu}$  angle,  $99.51(10)^\circ$ , are increased compared with those of complexes **1** and **2**. The bond angles  $\text{Cu–O(2)–N(2)}$  and  $\text{Cu–O(3)–N(2)}$  are  $108.1(3)$  and  $83.8(3)^\circ$  respectively. In general, the nitrite  $\text{O–N–O}$  angle observed for most  $\text{Cu}^{\text{II}}\text{–NO}_2$  complexes varies between  $110$  and  $125^\circ$ ,<sup>19,21</sup> and the angle  $\text{O(2)–N(2)–O(3)}$ ,  $114.1(3)^\circ$ , obtained for our complex **3** is well within this range.

### Magnetic properties

The X-band (9.81 GHz) powder EPR spectra at 300 K for the

**Table 3** Selected bond distances (Å) and angles (°) for complex **3**

Cu···Cu	2.9279(10)	Cu–O(1)	1.9054(22)
Cu···O(3)	2.495(3)	Cu–O(2)	1.9664(25)
Cu–N(1)	2.030(3)		
Cu–O(1)–Cu	99.51(10)	O(1)–Cu–O(1)	80.49(10)
N(1)–Cu–O(2)	98.59(11)	O(1)–Cu–O(2)	170.24(12)
Cu–O(2)–N(2)	108.1(3)	O(2)–N(2)–O(3)	114.1(3)

**Fig. 4** Plots of  $\chi_m$  (○) and  $\chi_m T$  (▽) versus  $T$  for complex **1**. The solid curve was calculated from equation (1) with  $2J = 81 \text{ cm}^{-1}$ ,  $g = 2.08$  (from EPR), and  $N\alpha = 60 \times 10^{-6} \text{ cm}^3 \text{ mol}^{-1}$ **Fig. 5** Plots of  $\chi_m$  (○) and  $\chi_m T$  (▽) versus  $T$  for complex **2**. The solid curve was calculated from equation (1) with  $g = 2.10$  (from EPR),  $2J = 25 \text{ cm}^{-1}$ , and  $N\alpha = 60 \times 10^{-6} \text{ cm}^3 \text{ mol}^{-1}$ 

complexes **1**, **2** and **3** exhibit a narrow isotropic resonance centred at  $g = 2.08$  for **1**,  $2.09$  for **2** and  $2.10$  for **3** respectively.

Variable-temperature magnetic studies were performed on dried, powder samples of complexes **1**, **2** and **3** in the temperature range 5–300 K. The magnetic data were fitted by the Bleaney–Bowers equation<sup>22</sup> (1) for a dinuclear copper(II)

$$\chi_m = [N\beta^2 g^2 / 3k(T - \theta)] [1 + \frac{1}{2} \exp(-2J/kT)]^{-1} (1 - \rho) + (N\beta^2 g^2 \rho / 4kT) + N\alpha \quad (1)$$

system where the symbols have their usual meanings. The best data fits (solid lines) for the complexes **1**, **2** and **3** are shown in Figs. 4, 5 and 6 respectively.

The temperature dependence of the molar magnetic susceptibility,  $\chi_m$  and  $\chi_m T$ , for complex **1** in Fig. 4 illustrates that at 300 K the  $\chi_m T$  value of  $0.71 \text{ cm}^3 \text{ K mol}^{-1}$  ( $\mu_{\text{eff}} = 2.49 \mu_B$ ) increases upon cooling, then reaches a rounded maximum at about 8 K with  $\chi_m T = 1.21 \text{ cm}^3 \text{ K mol}^{-1}$  and finally seems to decrease

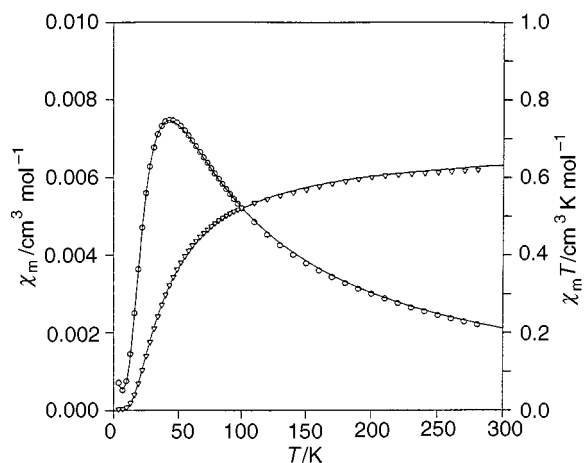


**Fig. 6** Plots of  $\chi_m$  ( $\circ$ ) and  $\chi_m T$  ( $\nabla$ ) versus  $T$  for complex **3**. The solid curve was calculated from equation (1) with  $g=2.09$  (from EPR),  $2J=-42\text{ cm}^{-1}$  and  $N\alpha=60\times 10^{-6}\text{ cm}^3\text{ mol}^{-1}$

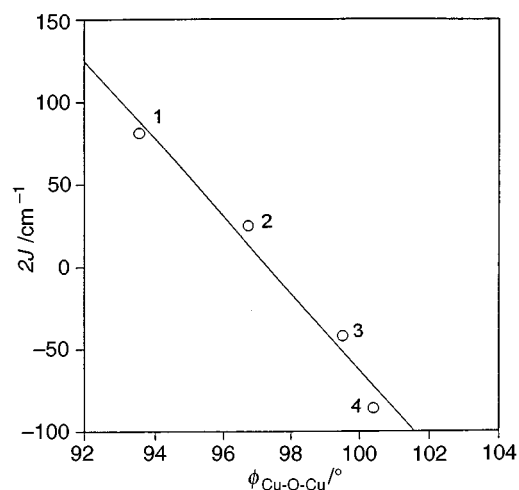


**Fig. 7** Plot of coupling constant ( $2J$ ) versus Cu-O-Cu angle,  $\phi$ , with a projected  $2J=0$  intercept at about  $97.3^\circ$  for complexes **1**, **2**, **3** and **4**

slightly below 8 K. Such behaviour reveals an intramolecular ferromagnetic interaction with a spin-triplet ground state. The decrease of  $\chi_m T$  below 8 K could be due to the weak intermolecular interaction. The best data fit by equation (1) gave  $2J=81\text{ cm}^{-1}$ ,  $g=2.08$  (from EPR data),  $\rho=0.017$ ,  $\theta=0.15\text{ K}$  and  $N\alpha=60\times 10^{-6}\text{ cm}^3\text{ mol}^{-1}$ . A similar data fit for a ferromagnetic exchange of **2** gave  $2J=25\text{ cm}^{-1}$ ,  $g=2.10$  (from EPR),  $\rho=0.021$ ,  $\theta=0.04\text{ K}$  and  $N\alpha=60\times 10^{-6}\text{ cm}^3\text{ mol}^{-1}$ .

The temperature dependence of  $\chi_m$  and  $\chi_m T$  for complex **3** is shown in Fig. 6. The  $\chi_m T$  value of  $0.62\text{ cm}^3\text{ K mol}^{-1}$  ( $\mu_{\text{eff}}=1.74\ \mu_{\text{B}}$ ) is lower than  $0.75\text{ cm}^3\text{ K mol}^{-1}$  ( $2.45\ \mu_{\text{B}}$ ) for a non-coupled two-spin ( $S_1=S_2=\frac{1}{2}$ ) system, indicating the likelihood of strong antiferromagnetic exchange. The  $\chi_m T$  value decreases upon cooling more quickly and approaches zero at about 10 K. The magnetic data, measured in the temperature range 5–300 K, were fitted by equation (1) giving  $2J=-42\text{ cm}^{-1}$ ,  $g=2.09$  (from EPR),  $\rho=0.001$ ,  $\theta=-8.61\text{ K}$  and  $N\alpha=60\times 10^{-6}\text{ cm}^3\text{ mol}^{-1}$ .

We now discuss the magnetic properties in a comparative fashion. The fitted  $2J$  values for the present complexes **1–3** and **4**<sup>12</sup> are 81, 25, -42 and  $-86\text{ cm}^{-1}$  respectively, and their corresponding mean Cu-O-Cu angles ( $\phi$ ) are 93.55, 96.77, 99.51 and  $100.4^\circ$  respectively. We have attempted to correlate the Cu-O-Cu angle,  $\phi$ , and the sign and magnitude of the magnetic coupling constant  $2J$ . A plot of  $\phi$  versus  $2J$  is shown in Fig. 7. Despite some scatter, the data points in Fig. 7 appear to conform to a reasonable straight line. In addition, Fig. 7 depicts an angular dependence which marks a crossover from antiferromagnetic to ferromagnetic coupling at a Cu-O-Cu

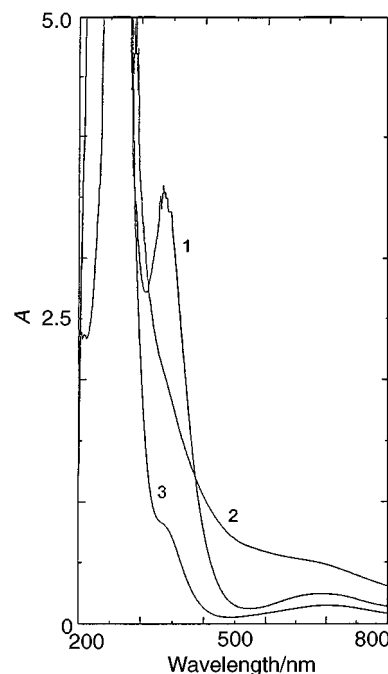


**Fig. 8** The UV/VIS absorption spectra of  $2\times 10^{-3}\text{ M}$  solutions (in methanol) of complexes **1**, **2** and **3**

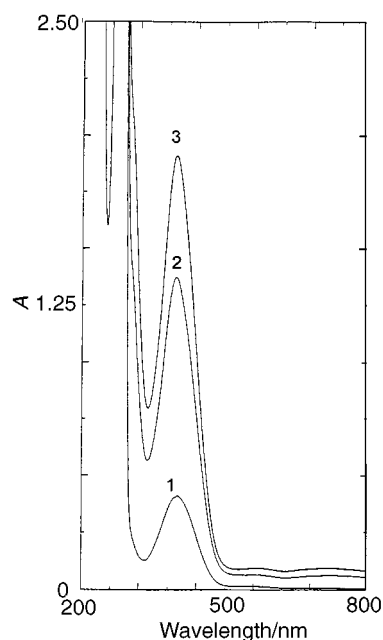


**Fig. 9** The UV/VIS spectra at 400 nm of  $5\times 10^{-5}\text{ M}$  solutions of the complexes **1**, **2** and **3** after addition of  $\text{H}_2\text{dtbc}$  (5 mM) in methanol. The spectra were recorded after 50 min

bridging angle of about  $97.3^\circ$ . This is close to the crossover point for bis( $\mu$ -hydroxo)-bridged dicopper(II) complexes, Cu-OH-Cu  $97.5^\circ$ .<sup>6</sup>

#### UV/VIS spectra and catalytic activity for the oxidation of $\text{H}_2\text{dtbc}$

The UV/VIS spectra (Fig. 8) of the  $2\times 10^{-3}\text{ M}$  solutions of the complexes **1**, **2** and **3** in methanol before addition of  $\text{H}_2\text{dtbc}$  were recorded in the range 200–800 nm. The much weaker low-energy region of the spectra at 680 nm is associated with the d-d transition. The high-energy region of the spectra is characterized by the occurrence of an intense band around 370 nm, which may be assignable to the ligand-to-metal charge-transfer (LMCT) bands. The  $\text{N}_3^-$  complex **1** shows the strongest band at 370 nm which may be assigned to the  $\text{N}_3^- \rightarrow \text{Cu}^{\text{II}}$  LMCT.<sup>23</sup> As shown in Fig. 9, 50 min after addition of  $\text{H}_2\text{dtbc}$  (5 mM) to

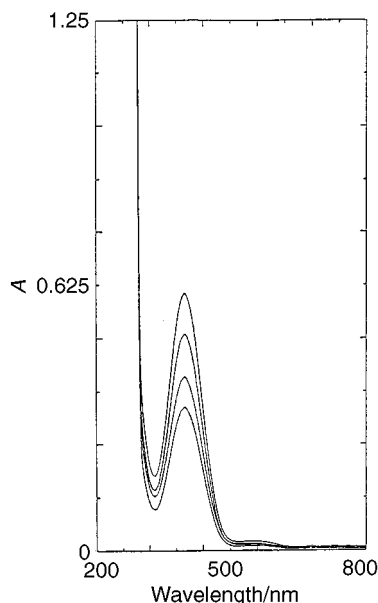


**Fig. 10** Increase of the quinone band at 400 nm after addition of  $\text{H}_2\text{dtbc}$  (5 mM) to a solution of complex **1** ( $5 \times 10^{-5}$  M) in methanol. The spectra were recorded every 10 min

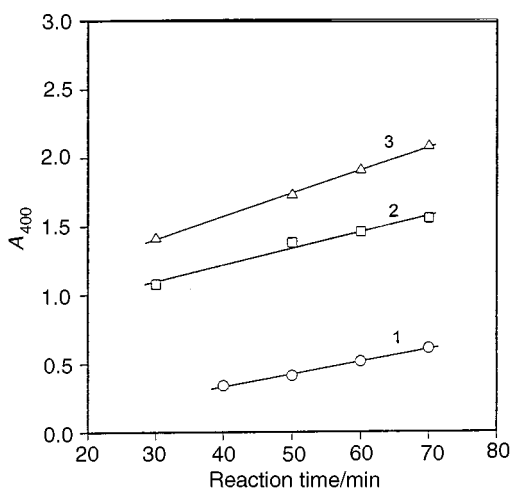


**Fig. 11** The linear increase in quinone absorption at 400 nm with reaction time for the addition of  $\text{H}_2\text{dtbc}$  (5 mM) to  $5 \times 10^{-5}$  M solutions of complexes **1**, **2** and **3**

solutions ( $5 \times 10^{-5}$  M) of the complexes **1**, **2** and **3** the LMCT band at about 370 nm and the d-d transition at 680 nm vanish. This indicates that the copper(II) complexes are reduced to copper(I) complexes. Simultaneously the quinone absorption at 400 nm appears. From their absorbances, which revealed that the order of catalytic activity towards the oxidation of  $\text{H}_2\text{dtbc}$  is  $3 > 2 > 1$ . Representative spectra for the course of the time-dependent increase of the quinone band are shown in Fig. 10. Overall the time dependence of the quinone absorption under the studied conditions for complexes **1-3** is linear (Fig. 11). These results revealed a catecholase activity order of  $1 < 2 < 3$ . This trend correlates to the Cu...Cu distances in complexes **1-3**: 2.8067(7) < 2.8690(22) < 2.9279(10) Å. The lower catecholase activity of the  $\text{N}_3^-$  complex **1** in the present system implies some inhibitory activity of  $\text{N}_3^-$  ion in the reaction. This is consistent with the finding that azide ion is an effective inhibitor in the structure and function of the copper binding sites of native metalloenzymes,<sup>1-4</sup> e.g. tyrosinase.

This study clearly established for the first time that the anionic  $\text{X}^-$  ligands of the complexes **1-3** are able to mediate significant changes for structural, magnetic coupling and catecholase activity.

## Acknowledgements

This research was supported by a grant (NCS86-2113-M-032-005) from the National Science Council of Taiwan.

## References

- Bioinorganic Chemistry of Copper*, eds. K. D. Karlin and Z. Tyeklar, Chapman & Hall, New York, London, 1993; T. G. Spiro, *Copper Proteins*, Wiley, New York, 1981; B. Reinhammer, in *Copper Proteins and Copper Enzymes*, CRC, Boca Raton, FL, 1984, vol. 3, pp. 1-35; E. I. Solomon, M. J. Baldwin and M. D. Lowery, *Chem. Rev.*, 1992, **92**, 521.
- K. A. Magnus, H. Ton-That and J. E. Carpenter, *Chem. Rev.*, 1994, **94**, 727.
- E. I. Solomon, in *Metal Clusters in Proteins*, ed. L. Que, American Chemical Society, Washington, DC, 1988, p. 116; N. Kitajima and Y. Moro-Oka, *Chem. Rev.*, 1994, **94**, 737; E. I. Solomon, U. M. Sundaram and T. E. Mackonkin, *Chem. Rev.*, 1996, **96**, 2563.
- M. Tremdiere and T. B. Bieth, *Phytochemistry*, 1983, **23**, 501; A. Rompel, H. Fischer, K. Büldt-Karentzopoulos, D. Meiwes, F. Zippel, H. F. Nolting, C. Hermes, B. Krebs and H. Witzel, *J. Inorg. Biochem.*, 1995, **59**, 715.
- Magneto-Structural Correlations in Exchange Coupled Systems*, eds. R. D. Willet, D. Gatteschi and O. Kahn, NATO ASI Ser. C, Reidel, Dordrecht, 1984, vol. 140.
- D. J. Hodgson, *Prog. Inorg. Chem.*, 1975, **19**, 173; V. H. Crawford, H. W. Richardson, J. R. Wasson, D. J. Hodgson and W. E. Hatfield, *Inorg. Chem.*, 1976, **15**, 2107.
- L. Merz and W. Hasse, *J. Chem. Soc., Dalton Trans.*, 1980, 875; M. Honda, N. Koga and S. Kida, *Bull. Chem. Soc. Jpn.*, 1988, **61**, 3853.
- T. Tokii, S. Nakahara, N. Hashimoto, M. Koikawa, M. Nakashima and H. Matsushima, *Bull. Chem. Soc. Jpn.*, 1995, **68**, 2533.
- K. S. Bürger, P. Chaudhuri and K. Wieghardt, *J. Chem. Soc., Dalton Trans.*, 1996, 247.
- L. K. Thomson, S. K. Mandal, S. S. Tandon, J. N. Bridson and M. K. Park, *Inorg. Chem.*, 1996, **35**, 3117.
- K. S. Bürger, P. Chaudhuri and K. Wieghardt, *Inorg. Chem.*, 1996, **35**, 2704.
- M. Mikuriya, M. Yamamoto and W. Mori, *Bull. Chem. Soc. Jpn.*, 1994, **67**, 1348.
- R. L. Carlin, *Magnetochemistry*, Springer, Berlin, 1986.
- E. J. Gate, Y. Le Page, J. P. Cherland, F. L. Lee and P. S. White, *J. Appl. Crystallogr.*, 1989, **22**, 384.
- N. Oishi, Y. Nishida, K. Ida and S. Kida, *Bull. Chem. Soc. Jpn.*, 1980, **53**, 2847; F. Zippel, F. Ahlers, R. Werner, W. Hasse, H. F. Nolting and B. Krebs, *Inorg. Chem.*, 1996, **35**, 3409.
- G. A. van Albada, M. T. Lakin, N. Veldman, A. L. Spek and J. Reedijk, *Inorg. Chem.*, 1995, **34**, 4910.
- R. Vicente, A. Escuer, E. Peñalba, X. Solans and M. Font-Bordia, *J. Chem. Soc., Dalton Trans.*, 1994, 3005.
- F. S. Stephens, *J. Chem. Soc. A*, 1969, 2081.
- F. Jiang, R. R. Conry, L. Bubacco, Z. Tyeklar, R. R. Jacobson, K. D. Karlin and J. Peisach, *J. Am. Chem. Soc.*, 1993, **115**, 2093.
- C. K. Johnson, ORTEP, Report ORNL-5138, Oak Ridge National Laboratory, Oak Ridge, TN, 1976.
- R. Allmann, S. Kremer and D. Juchacz, *Inorg. Chim. Acta*, 1985, **85**, L19; S. Takagi, M. D. Joesten and P. G. Lenhart, *J. Am. Chem. Soc.*, 1975, **97**, 444; K. A. Klanderman, W. C. Hamilton and I. Bernal, *Inorg. Chim. Acta*, 1977, **23**, 117.
- B. Bleaney and K. D. Bowers, *Proc. R. Soc. London, Ser. A*, 1952, **214**, 4519.
- M. E. Winkler, K. Lerch and E. I. Solomon, *J. Am. Chem. Soc.*, 1981, **103**, 7001.

Received 4th April 1997; Paper 7/02321I